Internal Report
DESY F15-83/03
October 1983

ARGUS AT HERA

Study of the Performance of an Existing Detector

by

H. Gennow and W. Schmidt-Parzefall

A R G U S at H E R A

Study of the Performance of an Existing Detector

H. Gennow
and
W. Schmidt-Parzefall

Abstract :

The performance of an upgraded version of the ARGUS detector now taking data at the DORIS e^+e^- storage ring has been studied. With a modest change of the detector we find that it would perform quite adequately for e-p collisions at HERA.
However, the performance depends mainly on the quality of the calorimeters to be added to the existing detector.

This study is not to be considered a proposal.

INTRODUCTION

For experimentation at HERA the use of existing detectors would be advantageous. In this note we study a possible upgrade of the existing detector ARGUS to meet the specific requirements for experiments at colliding electron and proton beams.

We will first shortly describe the existing detector and then outline the possible extension in section 2. In section 3 we define the kinematical variables and describe the simulation. The results are presented in section 4 and summarized in section 5.

I. THE ARGUS DETECTOR.

A view of the detector is shown in Fig. 1.
The most important data on its structure and performance are listed in Table 1.

TABLE 1

MAGNET		
	Field	8 kΓ
	Power	1.4 MW
	Weight	360 t
	Pole distance	2.9 m
	Inner coil radius	1.35 m
	Radius for tracking	0.95 m
DRIFT CHAMBER		
	Drift cell size	18 x 19 mm^2
	Number of drift cells	5940
	Number of layers	36
	Outer radius	0.83 m
	Numberof stereo layers	18
	Stereo angles	40 to 80 mrad
	Space resolution	200 μ
	dE/dx resolution	5% r.m.s.
	Momentum resolution	0.75% p + 0.5%

Time of Flight

Number of barrel counters	64
Number of end cap counters	2 x 48
Barrel radius	0,95 m
Time resolution	270 ps

Electromagnetic calorimeter

Number of barrel counters	1536
Number of end cap counters	2 x 352
Thickness of lead sheets	1 mm
Thickness of scintillator	5 mm
Radiatuion lengths	12,5
Energy resolution	7%/$\sqrt{E}$

Muon Identification

Absorption length of 1st filter	3.3
Absorption length of 2nd filter	1.8
Number of proportional tubes	2000

II. THE UPGRADING

For a Monte Carlo study a well defined input is needed. But the specific upgrading studied here is somewhat arbitrary. We consider it as a minimum of changes, which are almost unavoidable however other changes might eventually be proposed. The upgraded detector is shown in Fig. 2. The following components are changed :

a) The Electromagnetic Calorimeter

The present shower counters have 12.5 radiation lengths. By replacing the 1 mm thick lead sheets by 2 mm thick ones, the electromagnetic calorimeter has 25 radiation lengths and an energy resolution of 0.1/$\sqrt{E}$. This modification would take about 1 year, while the detector cannot be used. The capital investment is less than 0.5 MDM .

b) The Cylindric Drift Chamber

By the time HERA comes into operation, the present drift chamber will probably be worn out. However experience with the existing chamber is very satisfactory. Thus one would only rebuild the chamber but keep all the expensive

electronics and software.

To make efficient use of the existing space within the detector the new chamber would be magnified by 10% and a vertex chamber mechanically integrated. The track measurement could thus be extended from presently 65 cm to 85 cm, giving an improvement of a factor 1.7 for the momentum resolution. With an increased mechanical precision an overall improvement of the momentum resolution by a factor of 2 is feasable and σ_p/p^2 = 0.4% can be obtained.

c) Muon Identification and Barrel Hadron Calorimeter

The hadron filter has presently about 5 absorption lengths. Two more layers of absorbers and detectors are added, giving 9 absorption lengths in total. In addition, some crude hadron calorimetry is obtained with an energy resolution of 200%/$\sqrt{E}$.

d) End Cap Calorimeter

The quality of the detector for large Q^2 physics is mainly determined by the end cap calorimeter. It replaces the present end cap and covers a polar angle of up to 45^{o} around the outgoing proton beam. For optimum performance a Uranium calorimeter is foreseen, intermixed with iron to guide the magnetic flux. The energy resolution is 35% /$\sqrt{E}$. Sufficient granularity is achieved with 64 azimuthal x 14 polar bins amounting to 896 counters. The electromagnetic and hadron sections are read-out separately. A hole around the beam pipe passes small-angle particles to a foreward spectrometer. Around this hole the detector is insensitive. It can be shown that this dead region has almost no noticeable effect on large Q^2 physics.

e) Foreward Calorimeter

As far as possible away from the interaction point, a foreward calorimeter is placed to measure small angle particles. It is also made from Uranium absorbers and has an electromagnetic and a hadronic section.

f) Foreward Spectrometer

In between the end cap and the foreward calorimeters a system of track detectors will be placed. This is also useful for low Q^2 physics. In this study, however, only the performance of the upgraded detector with respect to large Q^2 physics is considered.

III. THE SIMULATION

The performance of the upgraded detector was studied by means of Monte Carlo generated neutral current (NC) and charged current (CC) events. For NC events the kinematics is determined by the scattered electron:

$$Q^2 = -q^2 = -(k-k')^2 = 2E_e E'_e (1-\cos\theta)$$

$$\nu = \frac{p \cdot q}{M_p} = E_p [2E_e - E'_e (1 + \cos\theta)]$$

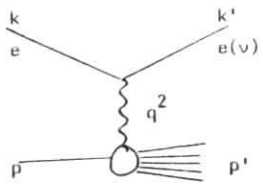

where k, k', p and p' denote

$k = (E_e, 0, 0, E_e)$

$k' = (E'_e\cos\theta, E'_e\sin\theta, 0, E'_e)$

$p = (-E_p, 0, 0, E_p)$

$p' = (-p_L^H, p_T^H, 0, E^H)$

For CC events the kinematical variables can only be measured through the hadronic system:

$$M_p \nu = E_p (E^H - E_L^H)$$

$$Q^2 = (P_T^H)^2 / (1 - \frac{E^H - P_L^H}{2E_e}) .$$

The scaling variables x and y and the invariant mass of the hadronic system are then given by

$$x = Q^2 / 2M_p \nu$$

$$y = 2M_p \nu / 4E_e E_p$$

$$W^2 = 2M_p - Q^2 + M_p^2$$

TABLE 3

Calorimeter	$\sigma/E \cdot \sqrt{E}$ Hadronic	E.M.
Forward spectrometer	.35	.15
Forward CAP	.35	.15
Barrel	2.	.10
Backward CAP	-	.12
	σ/P	
Driftchamber	$P \cdot 0.4\%$ $P \geq 2$ GeV	
	0.8% $P < 2$ GeV	
	Size of holes	
CAP's	ϕ = 17 cm	
Forward spectrometer	10 x 21 cm	

The essential input parameters to the Monte Carlo program are summarized in Table 2. The spatial resolution of the calorimeters has been parametrized according to the latteral size of the showers (see eg [1] and references therein).

Events generated according to the LUND model were processed through the Monte Carlo and then analysed in a separate program. Each particle was traced through the detector applying energy losses etc. For reasons of speed no shower simulation was made for particles reaching a calorimeter but instead the particles were stopped and the actual energy of the particles as well as the coordinates of the impact point were registered. The energy deposit in the calorimeter was obtained by smearing the energy of the particles by the resolution of the calorimeter.

The detector was devided into several parts (the various calorimeters + some other divisions) and the deposit energies were summed up and the

contributions to the total error in the kinematical variables were calculated by normal error propagation, thus allowing for an easy monitoring of the critical components of the detector.

IV. RESULTS

In Fig. 3 a(b) we give a schematic view of the relative importance of the detector components for the measurement of the kinematical variables x, y, Q^2 and ν for charched current events as visualized by the average energy (transverse momentum) seen by the different parts for two Q^2 ranges.

Due to obsured tracks the energy actually measured by the drift chamber (barrel region only) is on the average ~ 4% less than given in Fig. 3. This is illustrated in more detail in Table 3., where the fraction tracks found is plotted, and in Fig. 4, where the ratio of the reconstructed energy over the generated one is shown, in both cases for track angles > 30° and as function of x and y. In Fig. 5 we also show two examples of reconstructed events using the present reconstruction program without optimization for HERA events and without vertex fit.

TABLE 3 - Fraction found tracks in the driftchamber for track angles > 30°

		x			
y		0 - .25	.25 - .50	.50 - .75	.75 - 1.0
	.75 - 1.0	.98	.97	.96	.93
	.50 - .75	.98	.92	.89	.87
	.25 - .50	.96	.91	.99	1.0
	.0 - .25	.99	1.0	1.0	1.0

As seen from Fig. 3 the LUND model predicts a large fraction of neutrals (n, K^L_o), ~ 14%, for the barrel region compared to the average, ~ 5%, which will give rize to a tail in the distribution of the measured Q^2 in the case of no or poor barrel hadronic calorimeter. However, as seen from Fig. 6a-d where the ratio of the measured Q^2 over the generated one for CC events with $Q^2 > 10000$ $(GeV/c)^2$ is shown for the cases of no barrel calorimeter, one with 200% /$\sqrt{E}$, 35% / $\sqrt{E}$ and 0% / $\sqrt{E}$ energy resolution respectively, even a modest (200% / $\sqrt{E}$) calorimeter is helpful.

The errors in x and y due to smearing and imperfections are shown in Fig.7 as function of x and y for CC events. The error due to losses in the beam pipes has not been included and is shown separately. The latter error gives the limitation of an infinitely good detector in the event that no Monte Carlo corrections for the losses are tried. The error in Q^2 is likewise given in Table 4. In table 5 we give as well the errors in x and y for neutral current events, i.e. as measured by the scattered electron.

TABLE 4 - The relative error in Q^2 for CC events

σ E-res. + imperfections

		x			
		0. - .25	.25 - .50	.50 - .75	.75 - 1.0
y	.75 - 1.0	.75	.73	.84	.83
	.50 - .75	.26	.17	.081	.056
	.25 - .50	.12	.033	.024	.021
	.0 - .25	.076	.10	.13	.12

σ losses in beam pipes

		x			
		0. - .25	.25 - .50	.50 - .75	.75 - 1.0
y	.75 - 1.0	.55	.24	.16	.045
	.50 - .75	.44	.16	.066	.032
	.25 - .50	.50	.16	.078	.033
	.0 - .25	.77	.29	.13	.080

TABLE 5 - The errors in x (a) and y (b) for NC events. A 2% calibration error is assumed

a)

		x			
		.0 - .25	.25 - .50	.50 - .75	.75 - 1.0
y	.75 - 1.0	.0052	.012	.018	.025
	.50 - .75	.0068	.018	.027	.037
	.25 - .50	.013	.032	.050	.070
	.0 - .25	.064	.16	.22	.37

b)

		x			
		.0 - .25	.25 - .50	.50 - .75	.75 - 1.0
y	.75 - 1.0	.0045	.0037	.0034	.036
	.50 - .75	.012	.012	.011	.010
	.25 - .50	.021	.020	.019	.018
	.0 - .25	.031	.028	.026	.026

The impact of the measurement errors in $x(Q^2)$ and y on the structure function $F_2(x, Q^2)$ can be seen in Fig. 8 for various x-bins. Of interest is also the fragmentation function f(z), $z = E_{charged} / E_{C.J.}$, for the current jet and the measured distribution together with the ratio $f(z)^{meas.} / f(z)^{true}$ are given for two cuts on the current jet angle in Fig. 9a and b. In this context we also give the actually measured fractions of the total current jet energy as function of the transverse (P_T) and longitudinal (P_L) momentum of the jet. It is clear that there will be problems for any detector for the smaller angle jets, i.e. small P_T and large P_L since the jet fragments in that region to a large extent go in the beam pipes.

TABLE 6 - Fraction measured energy of the current jet.

$P_L^{C.J.}$ (GeV/c)

$P_T^{C.J.}$ (GeV/c)	0 - 50	50 - 100	100 - 150	150 - 250	250 - 400
120 - 160				.96	.99
80 - 120	.96	.92	.97	.92	.70
40 - 80	.95	.95	.93	.79	.52
0 - 40	.96	.88	.67	.54	.24

V. SUMMARY

We have studied the performance of an extended ARGUS detector, now placed at the DORIS e^+e^- colliding beam machine, at HERA.

The extentions mainly concern changes in the forward (proton) direction, more specifically replacement of the forward end cap by a Uranium calorimeter with iron plates for the magnetic return flux and the addition of a forward spectrometer, a U-calorimeter 5.5 m downstream of the interaction point with track chambers in front.

Such a detector should perform quite well in most of the kinematical range except possibly for a small corner at large current jet angles where a detector with a very good hadron calorimeter would be somewhat better off, but on the other hand this region in any case will have very limited statistics.

REFERENCES

1) U.Amaldi, Proceedings International Conference on Experimentation at LEP, Physica Scripta 23 (1981) 409.

FIGURE CAPTIONS

1. The present ARGUS Detector.
2. A possible extention of the ARGUS detector for HERA.
3. a) Average energy, b) average transverse momentum seen by the different components of the detector for two Q^2 ranges.
4. The ratio of reconstructed energy over generated energy in the drift-chamber for track angles > 30°.
5. Two reconstructed events for charged current events.
6. The ratio of the measured Q^2 over the generated Q^2 for CC events with $Q^2 > 10000\ GeV/c)^2$ for various qualities of the barrel hadron calorimeter: a) no calorimeter, b) 200% / $\sqrt{E}$ E-resolution, c) 35% / $\sqrt{E}$ E-resolution d) 0% /$\sqrt{E}$ E-resolution.
7. Errors on x and y for charged currents events. Losses in the beam pipes are not included but shown separately in b).
8. The ratio of the measured structure function $F_2(x,Q^2)$ over the true one for various x-bins.
9. The fragmentation function f(z), $z = E_{charged} / E_{C.J.}$, for the current jet for two different angular cuts: a) $\theta_{C.J.} > 30°$, b) $\theta_{C.J.} > 45°$.

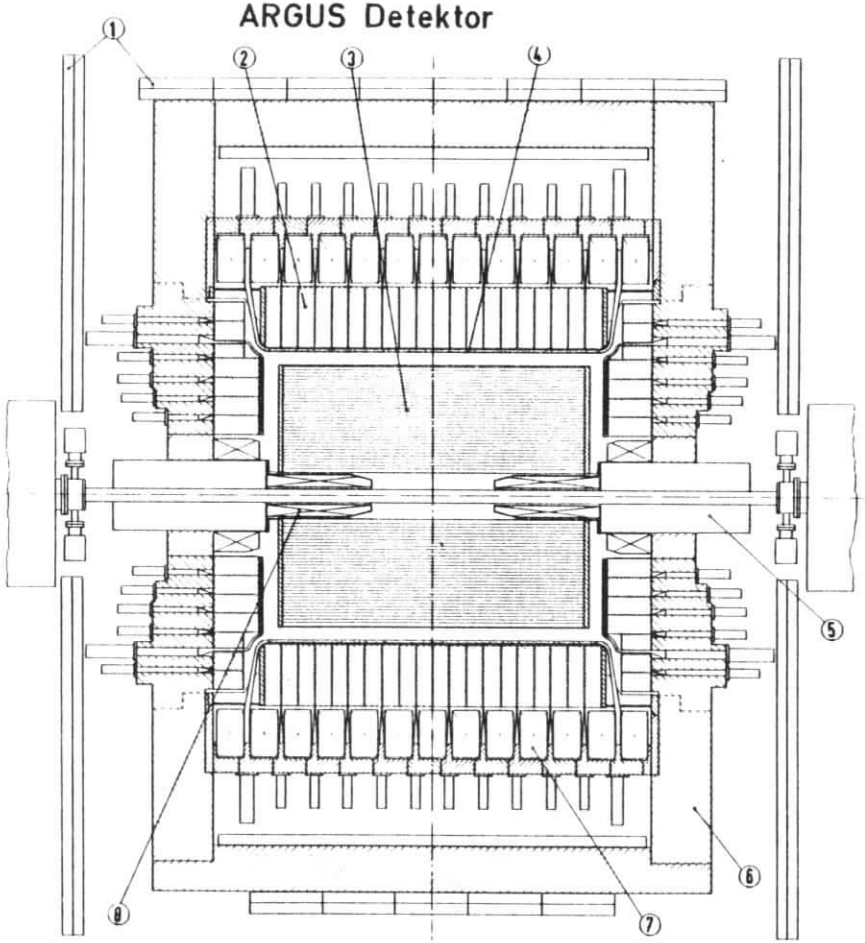

1.Myon Kammern	Muon chambers
2.Schauerzähler	Shower counters
3.Driftkammer	Drift chamber
4.Flugzeitzähler	Time of flight counters
5.Mini Beta Quadrupol	Mini beta quadrupole
6.Eisenjoch	Iron yoke
7 Hauptspule	Solenoid coils
8 Kompensationsspulen	Compensation coils

Fig 1

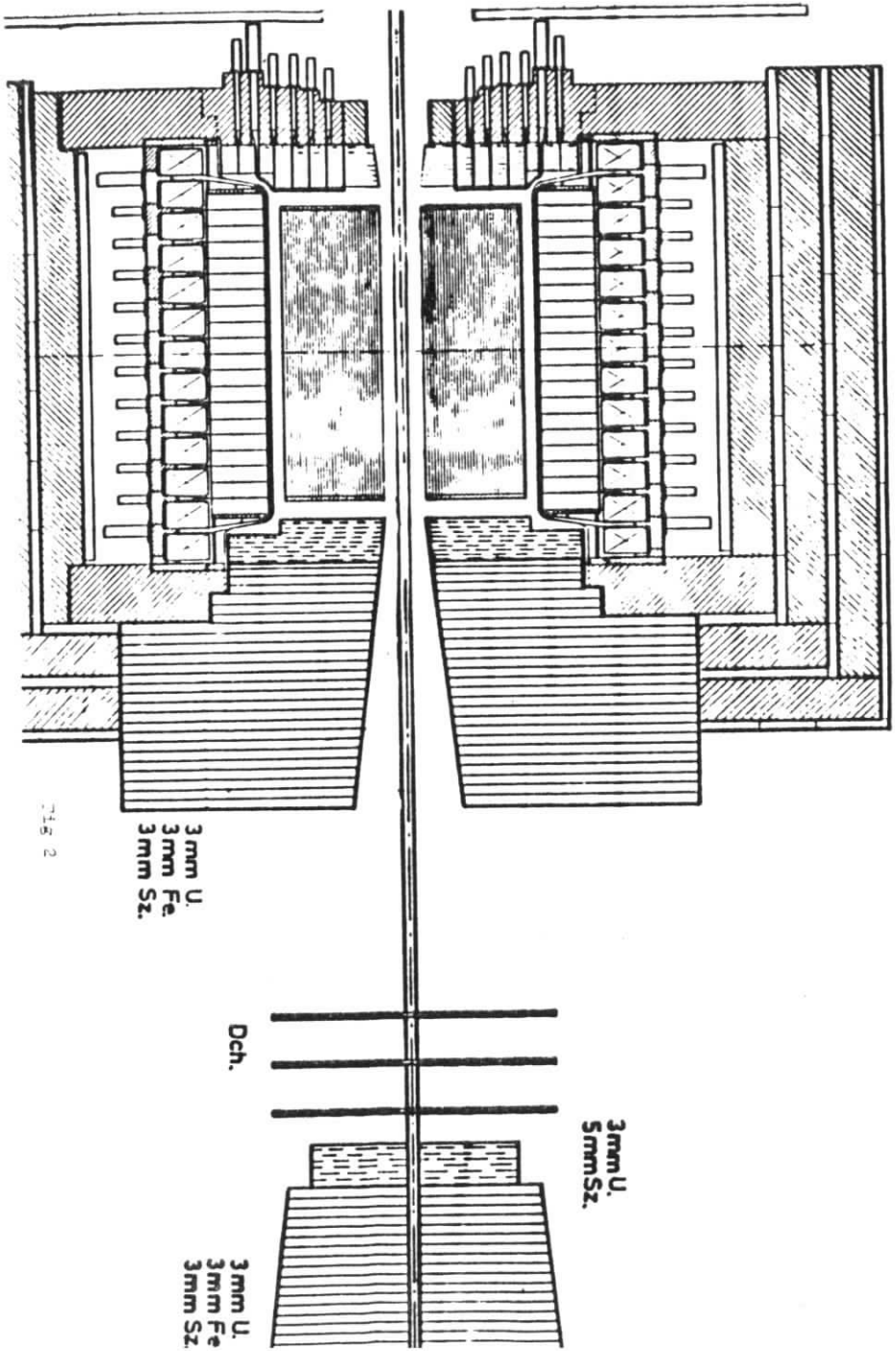
3 mm U.
3 mm Fe.
3 mm Sz.
Dch.
3mm U.
5mm Sz.
3 mm U.
3 mm Fe
3 mm Sz.

Fig 2

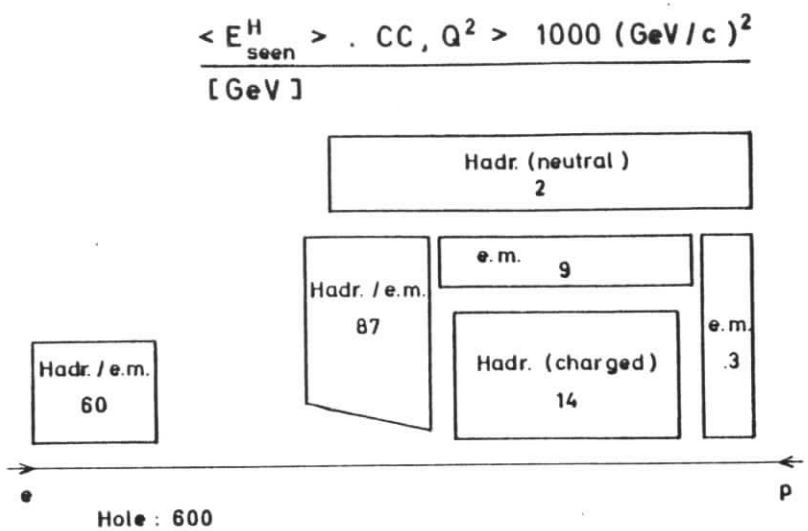
< E^H_seen > . CC, Q² > 1000 (GeV/c)²
[GeV]
Hadr. (neutral)
2
Hadr. / e.m.
87
e.m.
9
e.m.
.3
Hadr. (charged)
14
Hadr. / e.m.
60
e
p
Hole : 600

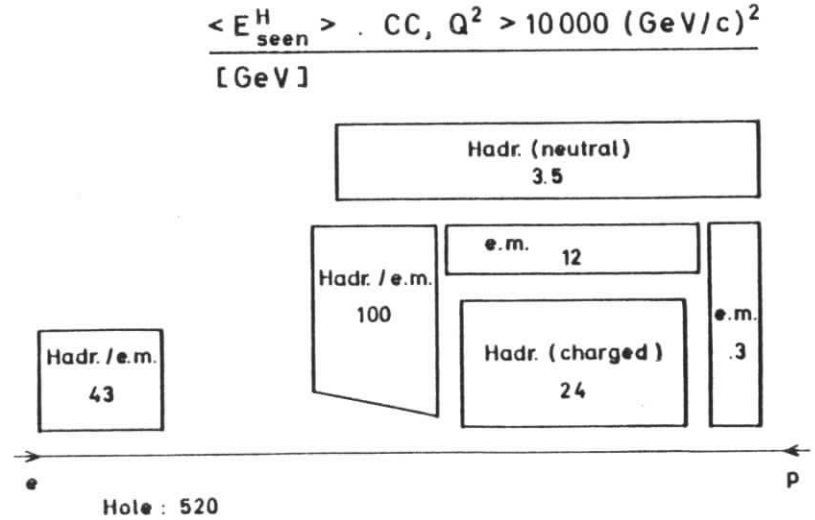
< E^H_seen > . CC, Q² > 10000 (GeV/c)²
[GeV]
Hadr. (neutral)
3.5
Hadr. / e.m.
100
e.m.
12
e.m.
.3
Hadr. (charged)
24
Hadr. / e.m.
43
e
p
Hole : 520

Fig 3a

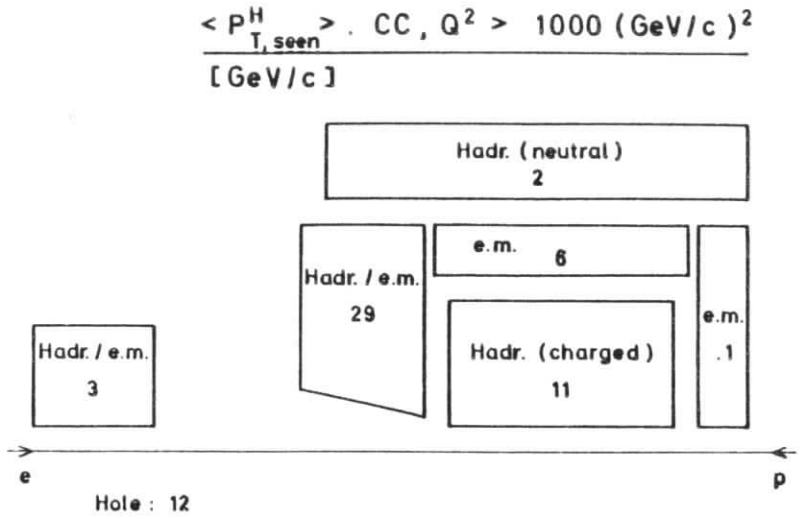
$< P^{H}_{T,seen} >$. CC, $Q^2 >$ 1000 (GeV/c)^2
[GeV/c]
Hadr. (neutral)
2
Hadr. / e.m.
29
e.m.
6
Hadr. / e.m.
3
Hadr. (charged)
11
e.m.
.1
e
p
Hole : 12

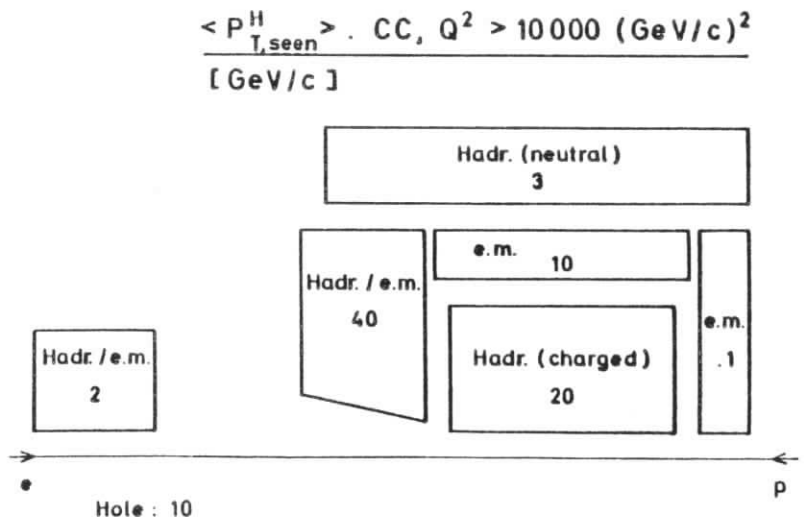
$< P^{H}_{T,seen} >$. CC, $Q^2 >$ 10000 (GeV/c)^2
[GeV/c]
Hadr. (neutral)
3
Hadr. / e.m.
40
e.m.
10
Hadr. / e.m.
2
Hadr. (charged)
20
e.m.
.1
e
p
Hole : 10

Fig 5b

E_{rec}/E_{gen}

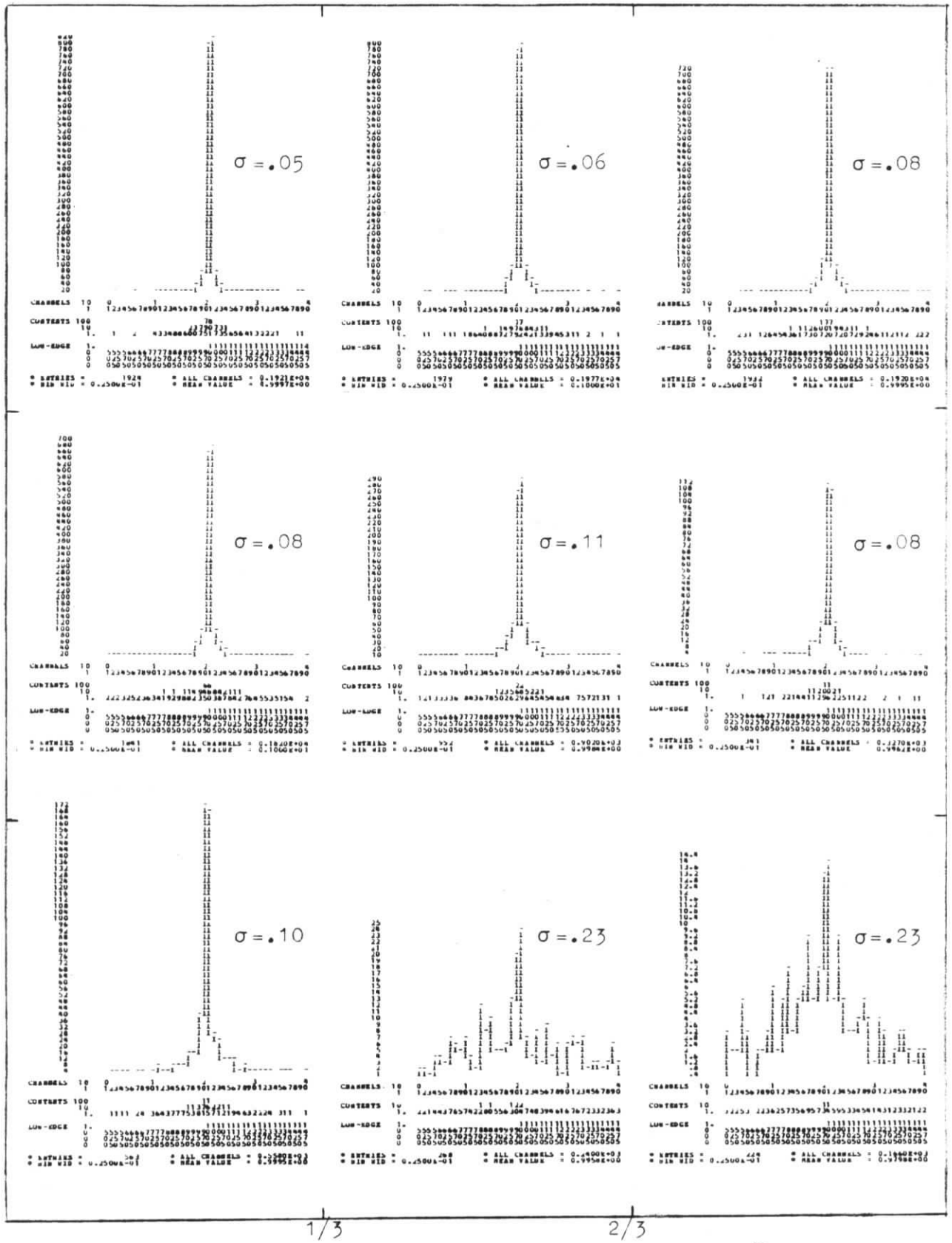

Fig 4

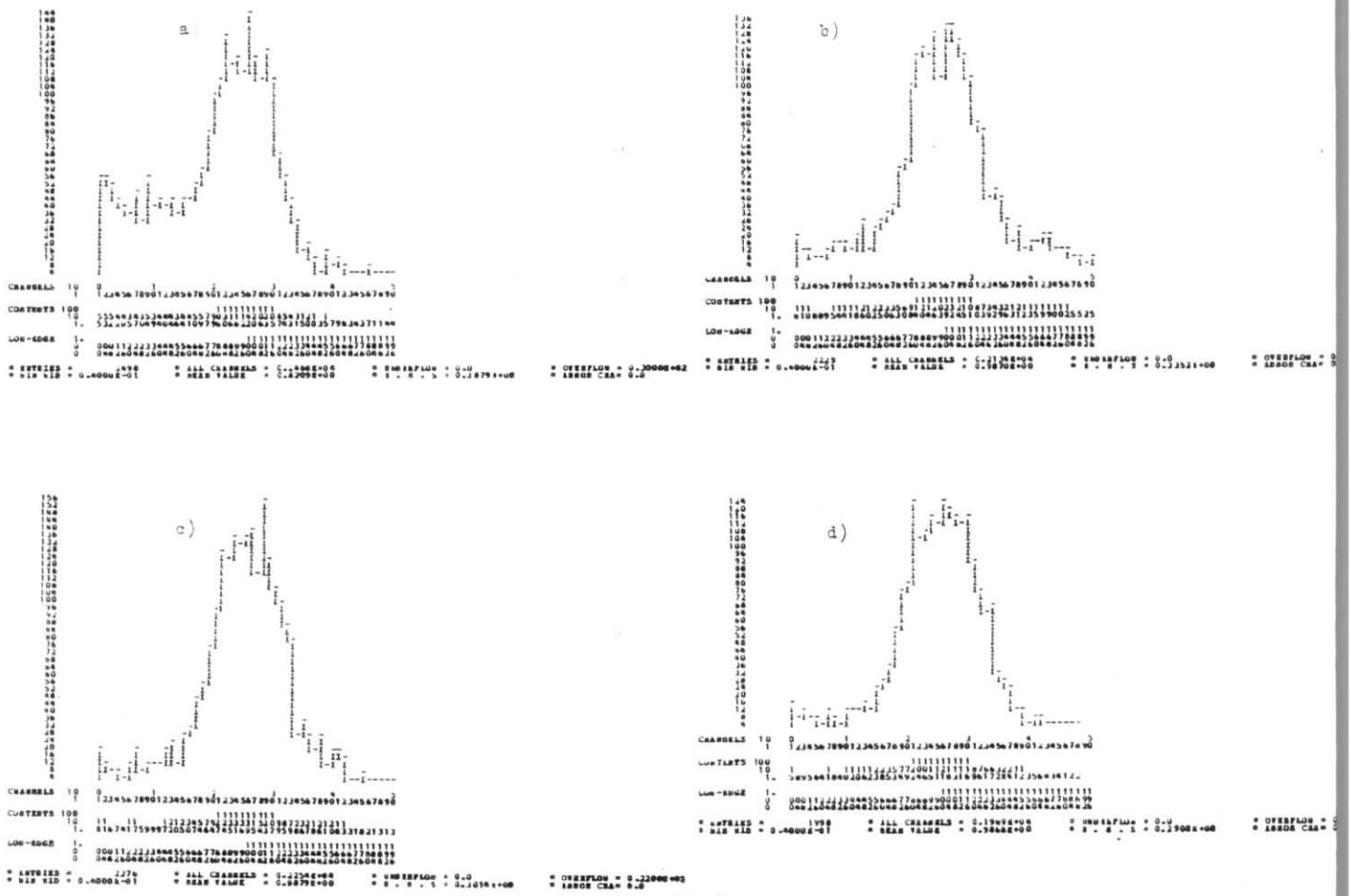

Fig 6

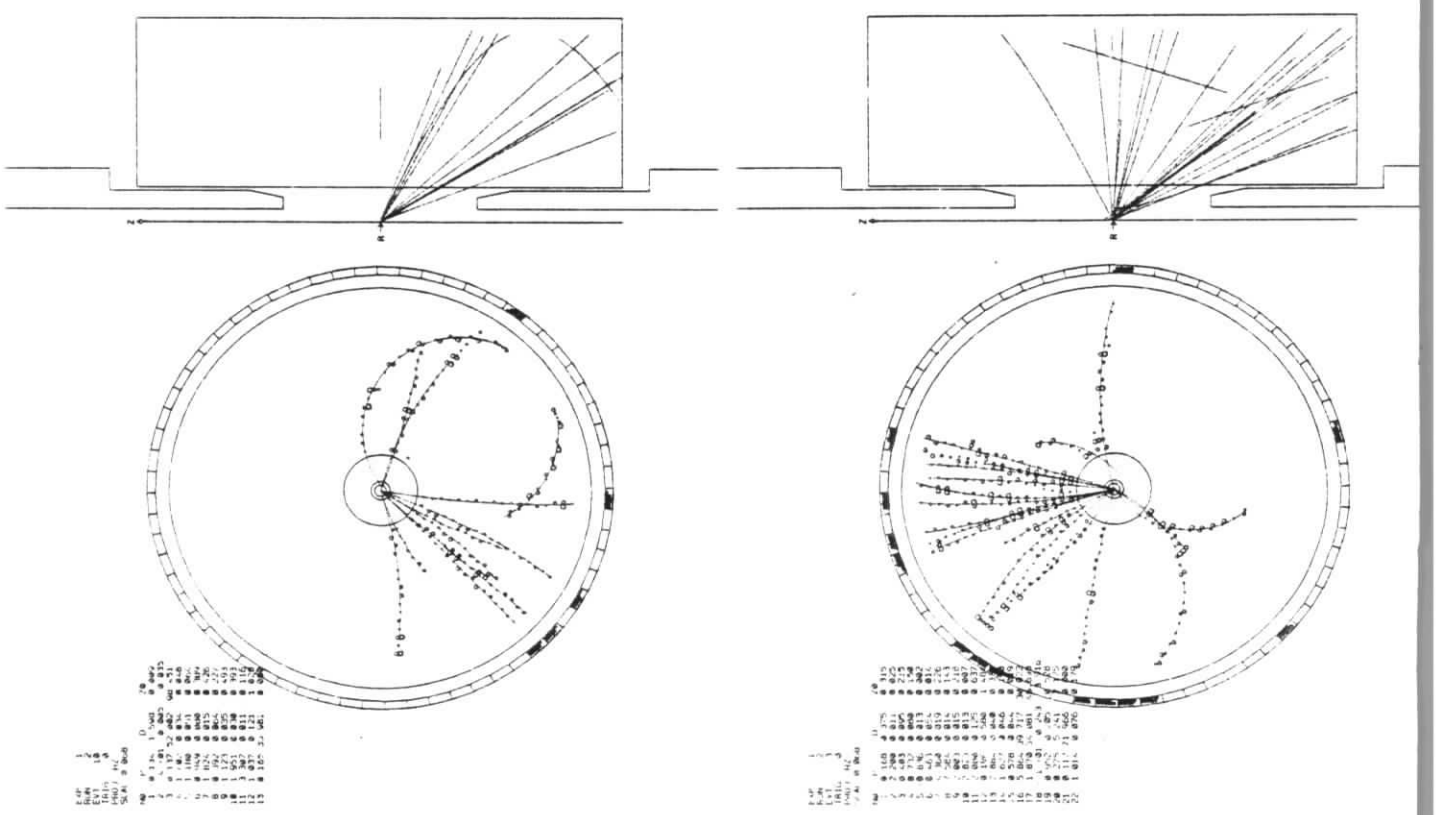

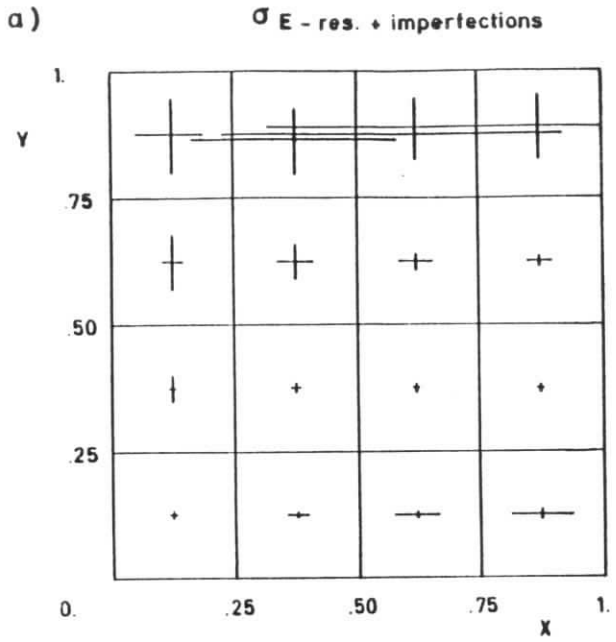
a)
σ E - res. + imperfections
Y
X
1.
.75
.50
.25
0.
.25
.50
.75
1.

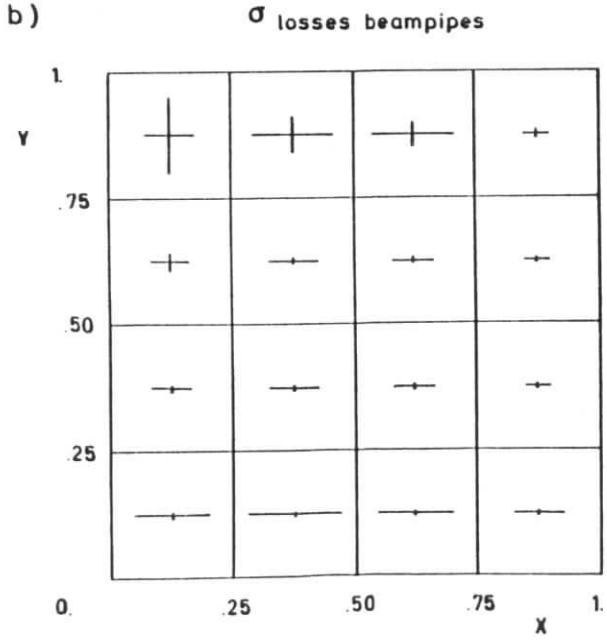
b)
σ losses beampipes
Y
X
1.
.75
.50
.25
0.
.25
.50
.75
1.

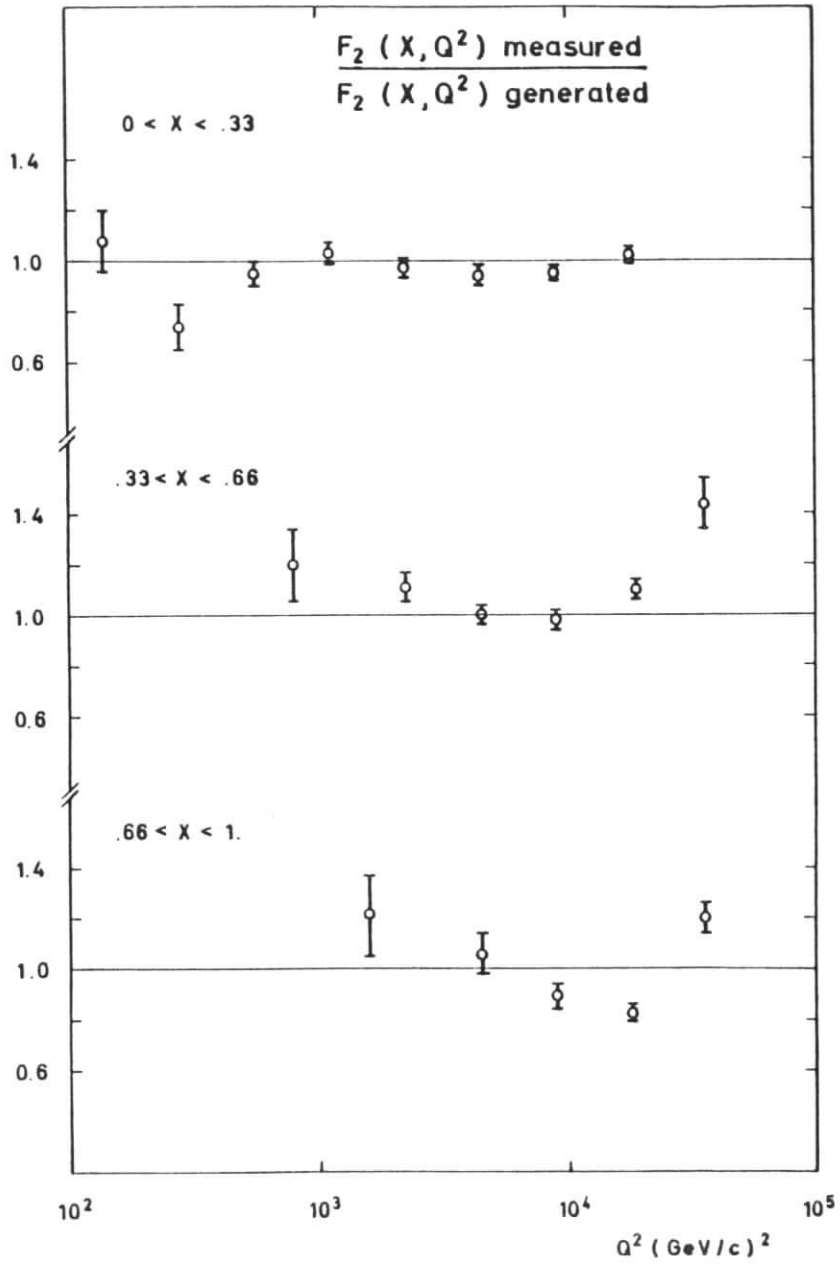
F2 (X, Q2) measured
F2 (X, Q2) generated
0 < X < .33
.33 < X < .66
.66 < X < 1.
1.4
1.0
0.6
10²
10³
10⁴
10⁵
Q² (GeV/c)²

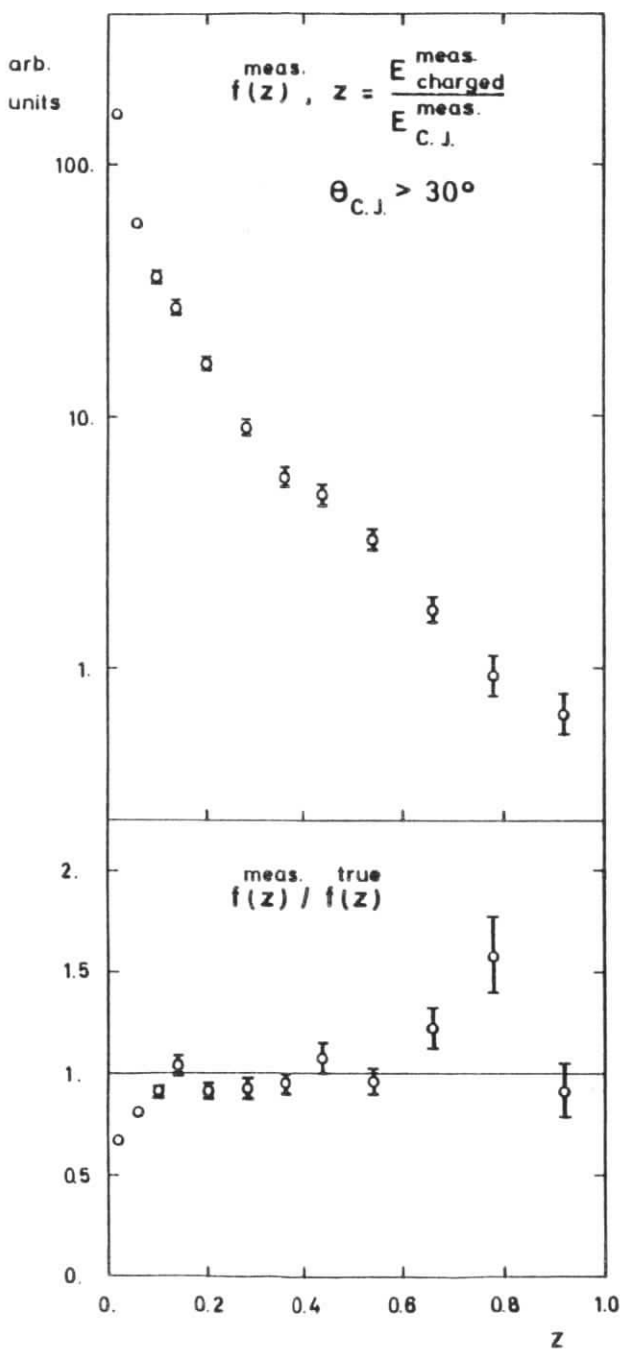
arb.
units
$f(z)^{meas.}$, $z = \frac{E^{meas.}_{charged}}{E^{meas.}_{C.J.}}$
$\theta_{C.J.} > 30°$
100.
10.
1.
$f(z)^{meas.} / f(z)^{true}$
2.
1.5
1.
0.5
0.
0.
0.2
0.4
0.6
0.8
1.0
z

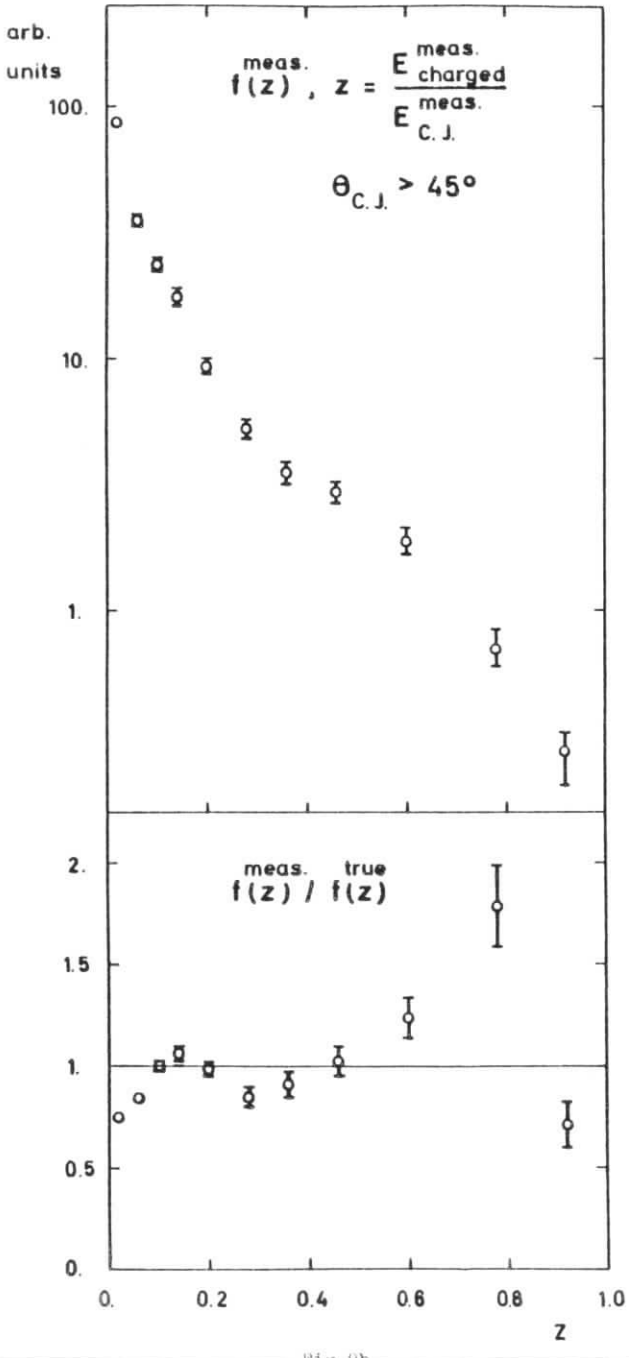
arb.
units
$f(z)^{meas.}$, $z = \frac{E^{meas.}_{charged}}{E^{meas.}_{C.J.}}$
$\theta_{C.J.} > 45°$
100.
10.
1.
$f(z)^{meas.} / f(z)^{true}$
2.
1.5
1.
0.5
0.
0.
0.2
0.4
0.6
0.8
1.0
z